Journal of Thermal Analysis, Vol. 40 (1993) 1123-1130

USE OF THERMOMAGNETOMETRY IN THE STUDY OF IRON-CONTAINING PYROTECHNIC SYSTEMS

M. E. Brown[*], *M. J. Tribelhorn and M. G. Blenkinsop*

CHEMISTRY DEPARTMENT, RHODES UNIVERSITY, GRAHAMSTOWN, 6140 SOUTH AFRICA

Thermal analysis is routinely used to characterize pyrotechnic fuels, oxidants and fuel/oxidant mixtures [1]. Thermomagnetometry (TM) can provide additional information if the magnetic properties of the materials change during reaction. TG, TM and DTA results for the iron/potassium permanganate, iron/barium peroxide, and iron/strontium peroxide systems as loose powders or pressed pellets indicate predominantly solid–gas mechanisms for reactions in these systems.

Keywords: pyrotechnic systems, DTA, TG, TM

Introduction

Amongst the iron-fuelled pyrotechnic systems which have received attention are $Fe/KMnO_4$, $Fe/K_2Cr_2O_7$ and Fe/BaO_2 [2–9]. Spice and Staveley [2] used a magnetic method to determine the iron content of several pyrotechnic systems after heating. From their observations on Fe/BaO_2 pellets, they proposed the occurrence of a pre-ignition reaction (PIR) and provided evidence for a solid–solid reaction mechanism. Nakahara [8, 9] concluded that the combustion wave in the Fe/BaO_2 system was preceded by flowing gas generated by decomposition of the oxidant. Hill and Wallace [5], reported a two-stage reaction in the $Fe/KMnO_4$ system.

In this study, thermomagnetometry (TM) [13, 14], as well as TG and DTA, have been used to re-examine the $Fe/KMnO_4$ and Fe/BaO_2 systems, and results for the Fe/SrO_2 system have also been obtained.

Experimental

Materials used were: iron powder (Johnson Matthey, <43 μm, 99.9% purity), BaO_2 (Unilab/Saarchem) and SrO_2 (Bernardy Chemie) (85% pure, <20 μm), and

---

[*] To whom correspondence should be addressed.

John Wiley & Sons, Limited, Chichester
Akadémiai Kiadó, Budapest

$KMnO_4$ (AECI Ltd, <53 μm). Fuel/oxidant compositions are given in mass percentages of fuel. Powders were mixed by tumbling and used either as powders, or as fragments broken from pressed (5 mm diameter, 1 ton pressure) pellets.

A Perkin-Elmer Delta Series TGA 7 and 1700 high-temperature DTA were used. The TG was calibrated using Curie points of nickel and iron. The magnet used was kept in position for thermomagnetometry. Platinum sample pans without covers were used. Difficulty was encountered in removing all traces of oxygen from the balance housing. Unless otherwise stated, the heating rate was 20 deg·min^{-1}.

Results and discussion

Oxidation of iron powder

The TM curve for Fe powder in N_2, after lengthy flushing, showed only the Curie transition of iron at 780°C. TG and TM curves for Fe powder in air are shown in Fig. 1. In the absence of a magnetic field (curve a), oxidation begins at about 150°C, accelerates to maximum rate at 550°C and approaches completion at 900°C at a mass gain of about 43.0% (calculated 42.9% for formation of Fe_2O_3, 38.2% for formation of Fe_3O_4). The TM curve (Fig. 1, curve b) shows a rapid apparent weight loss at ~570°C corresponding to the Curie point of Fe_3O_4. Fe_3O_4 is thus a major intermediate, probably formed in an O_2-deficient atmosphere at the metal/metal oxide interface. A magnetic event at ~340°C may arise from the formation on the surface of some ferromagnetic γ-Fe_2O_3 which converts to paramagnetic α-Fe_2O_3 at about this temperature. The increase in weight above 570°C corresponds to oxidation of Fe_3O_4 to Fe_2O_3.

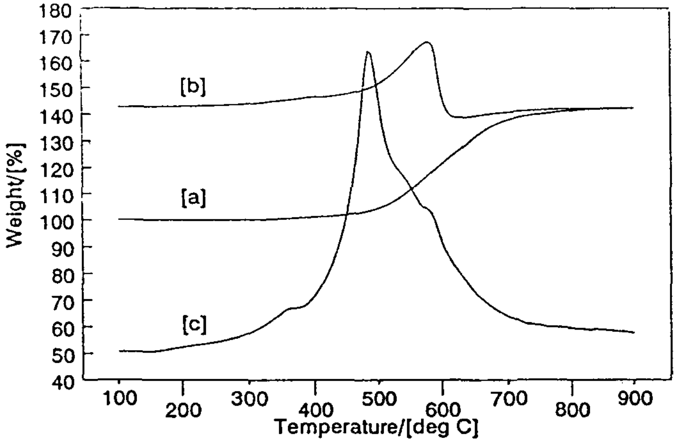

Fig. 1 Oxidation of Fe powder in air on heating at 20 deg·min^{-1}. (a) TG (b) TM (c) DTA

The DTA curve for Fe in air (Fig. 1, curve c) shows a broad complex exotherm, onset ~180°C, initial shoulder at ~300°C, and maximum at ~500°C.

Characterisation of the oxidants

KMnO4

TG (Fig. 2, curve a) and DTA (Fig. 6, curve a) curves showed the normal two-step decomposition (exothermic, onset ~290°C; endothermic, onset ~520°C).

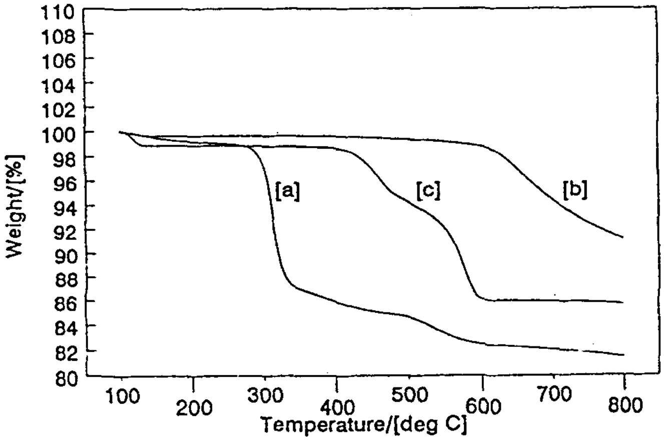

Fig. 2 TG of the oxidants in N_2 at 20 deg·min^{-1}. (a) $KMnO_4$ (b) BaO_2 (c) SrO_2

BaO2

TG curves in N_2 indicated removal of small amounts of moisture at ~100°C and onset of decomposition above 500°C and maximum rate at ~580°C with 7.7% mass loss (calculated 8.0% for decomposition of 85% pure BaO_2 to BaO and O_2) (Fig. 2, curve b). In O_2, onset of decomposition was shifted to ~650°C and the maximum rate to ~680°C. The DTA curve is shown in Fig. 6, curve b.

SrO2

Decomposition in nitrogen follows loss of adsorbed water (~1.1%) at 100°C and occurs in two steps. The first with mass loss ~4.0%, onset ~390°C, is followed by loss of a further ~8.0%, onset ~525°C (calculated 11.4% for decomposition of 85% pure SrO_2 to SrO and O_2). A further gradual loss of ~2% occurs towards the limit of the instrument at 900°C (decomposition of some $SrCO_3$?), (Fig. 2, curve c). In O_2, the relative mass losses in the two stages (8–9% followed by 3–4%) and the onset temperatures are dependent on the pressure of O_2. The DTA curve of SrO_2 in N_2 (Fig. 6, curve c) shows the onset of endothermic decomposition at ~350°C coinciding approximately with onset of oxidation of Fe in air (Fig. 1, curve a).

The pyrotechnic systems

Fe/KMnO4

The TG curve of 50% Fe/$KMnO_4$ powder in N_2 (Fig. 3, curve a) shows a first step (242°–262°C) corresponding to the first decomposition step of $KMnO_4$ (Fig. 2, curve a). The mass then begins to increase with temperature similarly to the TG curve of Fe in air (Fig. 1, curve a), becoming rapid above 540°C. The DTA curve of the powdered mixture in N_2 (Fig. 7, curve a) shows the onset of a large exotherm at around 540°C, assumed to indicate combustion. These features occur at about the same temperature as the second stage of the decomposition of $KMnO_4$. A small step in the TG curve prior to the accelerated mass gain is probably the result of simultaneous loss of oxygen from $KMnO_4$ and continued oxidation of Fe.

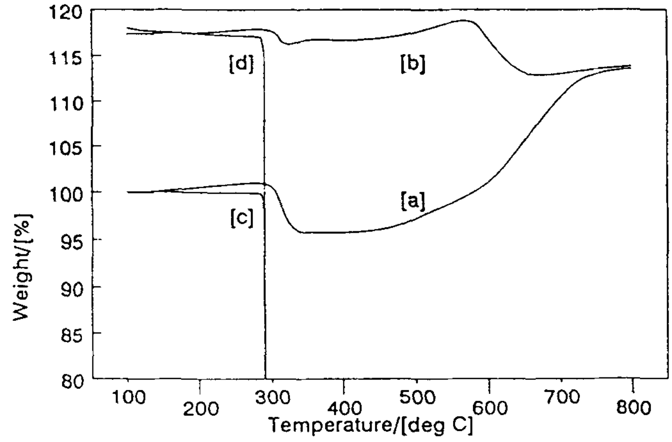

Fig. 3 TG and TM of the 50% Fe/$KMnO_4$ composition in N_2 at 20 deg·min^{-1}. (a) TG of powder (b) TM of powder (c) TG of pellet (d) TM of pellet

The total mass gain by the 50% Fe/$KMnO_4$ composition, on reaction, is ≈10% (calculated 21.5% for the 50% Fe oxidising to Fe_2O_3, and 7.0% loss for the decomposition of the 50% $KMnO_4$). The ~10% gain measured indicates incomplete oxidation of the Fe, but some participation of O_2(g) from the atmosphere in the TG housing.

TM curves of 50% Fe/$KMnO_4$ powder (Fig. 3, curve b) showed the two features characteristic of the oxidation of Fe in air, complicated by the simultaneous decomposition stages of $KMnO_4$.

TG and TM curves for pellets in N_2 (Fig. 3, curves c and d, respectively) showed that pellets exploded at about the onset temperature of $KMnO_4$ decomposition, probably due to a build-up of O_2 pressure.

These results indicate a solid–gas mechanism for reaction with the mixture in loose powder form, and probably also for reactions in pellets. Hill [5, 6] proposed parallel solid–gas and solid–solid mechanisms for the Fe/$KMnO_4$ system depending on the density of compaction of the sample.

Fe/BaO_2

Onset of oxidation of Fe in air (~400°C) (Fig. 1, curve a) coincides with the initial slow decomposition of BaO_2 (Fig. 2, curve b). The TG curve for 20% Fe/BaO_2 powder in N_2 (Fig. 4, curve a) shows both these processes. Oxidation of Fe by the product and residual O_2 is complete by ~650°C. The residual BaO_2 continues to decompose and at ~900°C the overall mass change is approaching the expected 2.2% gain for the simultaneous complete oxidation of Fe to Fe_2O_3 (calculated +8.6%) and decomposition of 85% pure BaO_2 to BaO (calculated –6.4%).

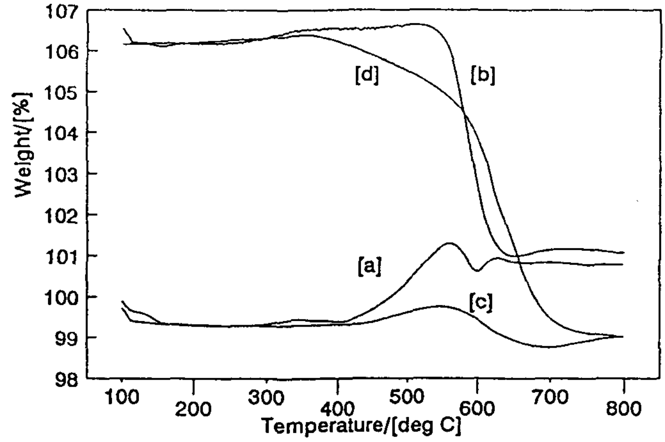

Fig. 4 TG and TM of the 20% Fe/BaO_2 composition in N_2 at 20 deg·min^{-1}. (a) TG of powder (b) TM of powder (c) TG of pellet (d) TM of pellet

The TM curve for 20% Fe/BaO_2 powder in N_2 (Fig. 4, curve b) shows features similar to the oxidation of Fe in air (Fig. 1, curve a) including the Curie transition of Fe_3O_4 at ~580°C. The DTA curve for 20% Fe/BaO_2 powder in N_2 (Fig. 7, curve b) shows overlapping exotherms with initial onset at ~400°C, but the major exotherm peaks at ~600°C . In O_2, the first exotherm is enhanced, but the second exotherm still predominates. There is an endotherm at ~830°C indicating decomposition of residual BaO_2.

The TG curve for a 20% Fe/BaO$_2$ pellet in N$_2$ shows only small mass changes up to 800°C (Fig. 4, curve c). TM shows that reaction has occurred by the Curie transition (broad) of Fe$_3$O$_4$ (Fig. 4, curve d).

Fe/SrO$_2$

TG results for Fe/SrO$_2$ powder differ from those for Fe/BaO$_2$ in that the decomposition of SrO$_2$ (Fig. 2, curve c) begins at lower temperatures than for BaO$_2$ (Fig. 2, curve b) and thus precedes the onset of oxidation of Fe (Fig. 1, curve a). The TG curve for 20% Fe/SrO$_2$ powder in N$_2$ (Fig. 5, curve a) shows a mass loss beginning at ~380°C which completely overshadows any concurrent oxidation of Fe. The slope of the curve is similar to that for the decomposition of SrO$_2$ alone in N$_2$. The oxidation of Fe becomes detectable through the slowing of the mass loss at about 480°C, i.e. well into the second stage of the decomposition of SrO$_2$, and by ~580°C a mass gain is observed with the overall mass change approaching a small loss of < 2.5% (which includes the initial water present) (calculated +8.6% for oxidation of the 20% Fe to Fe$_2$O$_3$, and –9.1% for decomposition of the 80% SrO$_2$ (85% pure) to SrO). The TM curve for 20% Fe/SrO$_2$ powder in N$_2$ (Fig. 5, curve b) shows a weight increase beginning at ~380°C, indicating formation of Fe$_3$O$_4$, followed shortly by the mass loss owing to decomposition of SrO$_2$. At ~570°C the Curie transition of Fe$_3$O$_4$ leads to a rapid apparent loss of weight. The DTA curve of 20% Fe/SrO$_2$ powder in N$_2$ (Fig. 7, curve c) shows an initial fairly strong endotherm, onset ~400°C, rapidly overlapped by a complex series of exotherms with two sharp maxima (~520°C and ~650°C).

The TG curve of a 20% Fe/SrO$_2$ pellet (Fig. 5, curve c) showed a smooth mass loss with onset temperature corresponding to decomposition of SrO$_2$ and mass loss approximately that expected for decomposition of SrO$_2$ alone. TM (Fig. 5, curve d) indicated some oxidation of the Fe.

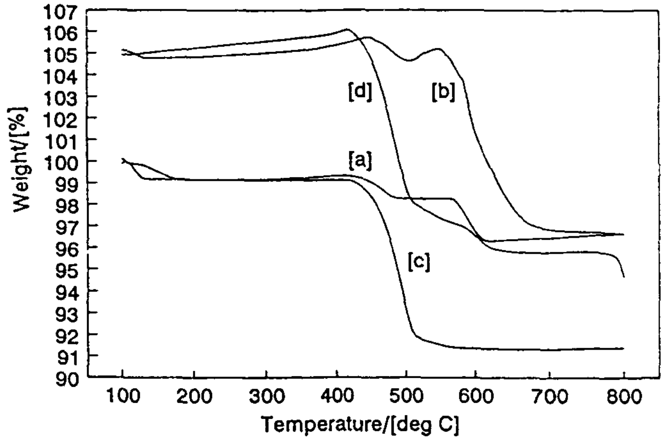

Fig. 5 TG and TM of the 20% Fe/SrO$_2$ composition in N$_2$ at 20 deg·min^{-1}. (a) TG of powder (b) TM of powder (c) TG of pellet (d) TM of pellet

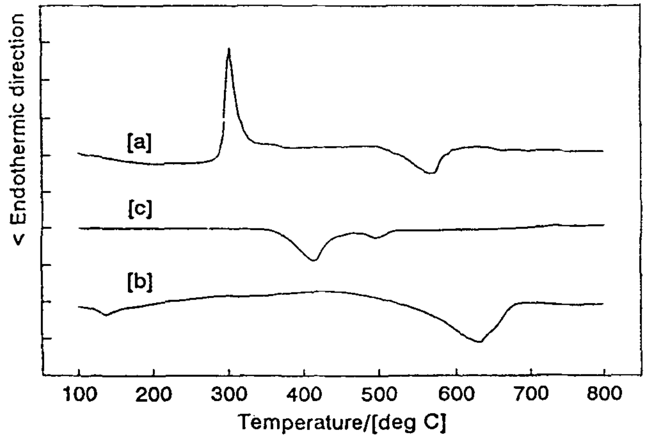

Fig. 6 DTA of the oxidants in N_2 at 20 deg·min^{-1}. (a) $KMnO_4$ (b) BaO_2 (c) SrO_2

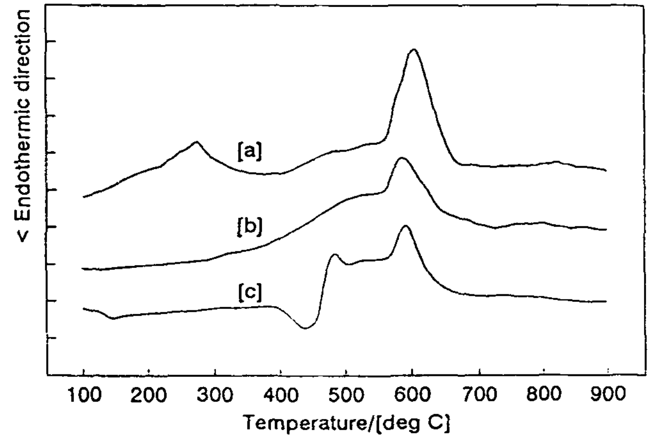

Fig. 7 DTA of the pyrotechnic systems (powders) in N_2 at 20 deg·min^{-1}. (a) 50% Fe/$KMnO_4$ (b) 20% Fe/BaO_2 (c) 20% Fe/SrO_2

Conclusions

It is important in industrial applications of pyrotechnics to ascertain whether reactions occur in the condensed phase, or with participation of gas formed by prior decomposition of the oxidant. Thermomagnetometry (TM) can provide information on the mechanism if the magnetic properties of some of the materials change during the course of reaction. TM has been used in this study to examine some pyrotechnic systems with iron powder as fuel and potassium permanganate, or barium peroxide, or strontium peroxide as oxidant.

The TG curves for the oxidation of Fe show a final mass gain corresponding to the formation of Fe_2O_3 as expected. TM shows the Curie point of Fe_3O_4 at around 570°C. A magnetic event at ~340°C probably arises from the surface formation of some ferromagnetic γ-Fe_2O_3 which converts to paramagnetic α-Fe_2O_3 at about this temperature.

TG curves for all three Fe/oxidant systems, heated in powder form at 20 $\mathrm{deg \cdot min^{-1}}$ in N_2, showed superimposition of the oxidation of Fe on the decompositions of the oxidants. DTA traces showed strongly exothermic processes corresponding to ignition. The TM traces showed the same features as that of Fe in air, suggesting that reaction under these conditions is solid–gas with little or no interaction between Fe and the solid oxidants. In some mixtures the presence of unreacted Fe was apparent from the Curie transition at 780°C.

Fe/oxidant pellets behaved differently from loose powders, but there was no conclusive evidence for solid–solid reaction mechanisms. Most of the observations could be explained by trapping of the gaseous products of oxidant decomposition within the pellets.

References

1 P. G. Laye and E. L. Charsley, Thermochim. Acta, 120 (1987) 325.
2 J. E. Spice and L. A. K. Staveley, J. Soc. Chem. Ind. 68 (1949) 313, 348.
3 G. Rees, Fuel, 52 (1973) 138.
4 R. A. W. Hill, Proc. Roy. Soc., 226A (1954) 455; Trans. Far. Soc., 53 (1957) 1136.
5 R. A. W. Hill and A. A. Wallace, Nature, 178 (1956) 692.
6 R. A. W. Hill and J. N. Welsh, Trans. Far. Soc., 55 (1959) 299.
7 F. Booth, Trans. Far. Soc., 49 (1953) 272.
8 S. Nakahara, J. Ind. Expl. Soc. Japan, 22(5) (1961) 259.
9 S. Nakahara and T. Hikita, J. Ind. Expl. Soc. Japan, 20(5) (1959) 356, 21(1) (1960) 2.
10 S. St. J. Warne and P. K. Gallagher, Thermochim. Acta, 110 (1987) 29.
11 S. St. J. Warne, H. J. Hurst and W. I. Stuart, Thermal Analysis Abstracts, 17 (1988) 1.

Zusammenfassung — Thermoanalyse wird routinemäßig zur Beschreibung von pyrotechnischen Brennstoffen, Oxydanten und Brennstoff/Oxydant-Gemischen eingesetzt. Thermomagnetometrie kann zusätzliche Informationen liefern, wenn sich die magnetischen Eigenschaften des Stoffes während der Reaktion verändern. TG-, TM- und DTA-Ergebnisse für Eisen/Kaliumpermanganat-, Eisen/Bariumperoxid und Eisen/Strontiumperoxid-Systeme (in Pulver- oder Preßpelletform) zeigen vorwiegend Feststoff-Gas-Mechanismen für die Reaktionen in diesen Systemen.